

Optimality of the Heating-Rate-Constrained Aerocruise Maneuver

I. Michael Ross* and John C. Nicholson†

U.S. Naval Postgraduate School, Monterey, California 93943

A synergetic maneuver can accomplish orbital plane changes with less fuel than an exoatmospheric maneuver. During the atmospheric pass, the spacecraft is subjected to very high heating rates, and any extra thermal protection required may offset the fuel savings. A heating-rate-constrained synergetic maneuver called aerocruise has been widely studied as a means for lowering the weight of the thermal protection system. We question the optimality of the aerocruise maneuver by considering the necessary and sufficient condition for a trajectory to remain on the heating-rate boundary. By replacing the aerocruise-powered turn by a maximum thrust maneuver that we call aerobang, a perturbed synergetic maneuver is obtained. This maneuver is compared against the numerically optimized aerocruise maneuver for the entry research vehicle. The results demonstrate that the aerobang maneuver consistently yields improved performance, i.e., inclination change per fuel mass, over the aerocruise maneuver by as much as 14%. This result indicates that the optimal synergetic maneuver is yet to be determined and could very well be more complicated than a simple aerocruise turn.

Nomenclature

| | |
|-----------------|---|
| a_s, a_n, a_w | = nongravitational perturbing accelerations on the vehicle in the tangential, normal, and binormal directions, respectively |
| C | = constant multiplier associated with an aerodynamic heating-rate model |
| C_D | = drag coefficient |
| C_L | = lift coefficient |
| D | = aerodynamic drag force |
| f | = generic state constraint |
| g | = inverse-square gravitational acceleration, μ/r^2 |
| L | = aerodynamic lift force |
| M | = speed exponent of the aerodynamic heating-rate model |
| m | = mass of the space vehicle |
| N | = atmospheric density exponent of the aerodynamic heating-rate model |
| $q; q_{\max}$ | = aerodynamic heating rate on the spacecraft; maximum value |
| $\mathbf{r}; r$ | = position vector of the spacecraft from the Earth's center; its magnitude |
| $T; T_{\max}$ | = magnitude of the thrust force; maximum value |
| $\mathbf{v}; v$ | = inertial velocity of the spacecraft; its magnitude |
| v_e | = exhaust speed of the power plant |
| α | = angle of attack |
| β | = exponential scale factor of a local atmospheric density model |
| γ | = flight-path angle |
| δ | = bank angle |
| θ | = longitude |
| ξ | = heating-rate parameter, $\beta N/M$ |
| $\rho; \rho_0$ | = atmospheric density; reference value |
| φ | = latitude |
| ψ | = heading angle |

Introduction

ORBITAL plane changes require very large characteristic velocities; in fact, a single-impulse, 60-deg plane change requires as

much delta- V as that required to place a satellite in low Earth orbit.¹ A synergetic maneuver^{1–4} uses atmospheric forces to assist in orbital plane changes and is an alternative to the use of a purely propulsive maneuver. It holds the potential for substantial fuel savings and could be an important maneuver for a future transatmospheric vehicle, including a military space plane. If a synergetic maneuver is to be superior to an all-propulsive one, it is desirable that the vehicle's lift-to-drag ratio L/D be significantly higher than 1.0 (Ref. 3). However, high- L/D vehicles experience very high integrated heat loads ($\sim 10^9$ J/m²) (Ref. 3), and they produce high stagnation-point heating rates ($> 10^6$ W/m²) (Ref. 5). Left unconstrained, a high thermal load requires a heavy thermal protection system that would offset any savings in propellant. Thus, a constraint on the thermal load is vital for defining the optimal synergetic maneuver.

When thermal constraints are imposed on the vehicle, the synergetic maneuver has lower efficiency because the bank angle must be modulated to keep the temperature limits within bound. Recent research^{6–8} indicates that the flight over the heating-rate-constrained arc requires substantially more analysis than previously thought.⁹ One issue^{6,7} is whether nontrivial touch points occur for optimal synergetic maneuvers, as some prior numerical studies⁹ seem to indicate. A related question is the optimality of the constrained arc itself when it is not a touch point. The aerocruise maneuver is one such constrained arc that has been widely studied.^{9–11} By definition, the aerocruise maneuver is accomplished by continuous thrusting to balance aerodynamic drag. From a trajectory optimization point of view, there is no theoretical justification for this thrust program. Because proofs of global optimality are difficult tasks, some questions on optimality may be resolved by numerical analysis. For instance, if a single numerical example were to demonstrate that an alternative synergetic maneuver consumes less propellant than the aerocruise maneuver, it would disprove the optimality of aerocruise, strengthening prior theoretical conjectures.^{6,7} The parametric study of Ref. 12 indicates that a maximum-thrust maneuver called aerobang may just be this alternative synergetic maneuver that yields improved performance; however, that analysis was limited to the atmospheric portion of the maneuver. In this paper, we analyze the full maneuver after laying the groundwork for control profiles over the constrained states. After numerically optimizing the aerocruise maneuver for a given heating-rate constraint, the aerocruise portion of the maneuver is then replaced by a maximum-thrust arc, i.e., aerobang, while maintaining the same heating rate. This substitution of a portion of the maneuver is akin to performing a control variation and evaluating the direction of the change in the cost. The study shows that this aerobang maneuver consistently yields improved fuel performance.

Received Feb. 26, 1997; revision received Feb. 3, 1998; accepted for publication Feb. 3, 1998. This paper is declared a work of the U.S. Government and is not subject to copyright protection in the United States.

*Assistant Professor, Department of Aeronautics and Astronautics, Mail Code AA-Ro. Senior Member AIAA.

†Graduate Student, Department of Aeronautics and Astronautics; Lieutenant, U.S. Navy.

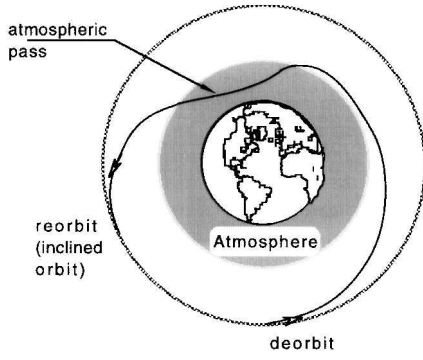


Fig. 1 Schematic of a synergetic maneuver.

Before proceeding any farther, a word of caution is in order. Because the major objective of this research was to perturb the aerocruise maneuver (and thereby determine the direction of the change in the cost index, viz., fuel), the models chosen (vehicle, atmosphere, etc.) were simple enough that the focus was on the key issues of trajectory performance. Thus, complexities such as variations in the aerodynamic coefficients arising due to the changes in the flow regimes the vehicle encounters as it passes from a free molecular flow to a hypersonic continuum regime were completely ignored.

Background

The basic synergetic maneuver (Fig. 1) begins with a retrorocket burn that lowers the perigee well into the atmosphere. During the atmospheric pass, the vehicle is banked so that the lift vector is in a lateral direction, thus producing an aerodynamic turn. This turn may be accomplished with or without any thrusting. In this paper we are concerned with the powered turn maneuver. The optimality of the glide maneuver has been discussed by Seywald.⁷ Following the aerodynamic turn, the vehicle is reboosted to the desired orbital altitude with an additional rocket burn to circularize the orbit.

The equations of motion for such an aerospace vehicle are well known¹³ and may be written in spherical coordinates:

$$\dot{r} = V \sin \gamma \quad (1a)$$

$$\dot{\theta} = \frac{V \cos \gamma \cos \psi}{r \cos \varphi} \quad (1b)$$

$$\dot{\phi} = \frac{V \cos \gamma \sin \psi}{r} \quad (1c)$$

$$\dot{v} = a_s - g \sin \gamma \quad (1d)$$

$$\dot{\psi} = \frac{a_w}{V \cos \gamma} - \frac{V}{r} \cos \gamma \cos \psi \tan \varphi \quad (1e)$$

$$\dot{\gamma} = \frac{a_n}{V} - \left(g - \frac{V^2}{r} \right) \frac{\cos \gamma}{V} \quad (1f)$$

$$\dot{m} = -\frac{T}{V_e} \quad (1g)$$

The nongravitational perturbing accelerations on the vehicle are given by¹³

$$a_s = \frac{T \cos \alpha - D}{m} \quad (2)$$

$$a_n = \frac{(L + T \sin \alpha) \cos \delta}{m} \quad (3)$$

$$a_w = \frac{(L + T \sin \alpha) \sin \delta}{m} \quad (4)$$

Note that the thrust vector is assumed to be fixed along the reference body axis of the vehicle from which α is measured. For simplicity, thrust vector control, i.e., a gimbaled system, is not considered here.

Effect of a Heating-Rate Constraint

Because the allowable thermal load on the vehicle is fundamentally a state constraint, \mathbf{r} and \mathbf{v} are required to satisfy

$$f(\mathbf{r}, \mathbf{v}) \leq 0 \quad (5)$$

If a trajectory hits the boundary of this region, i.e., $f(\mathbf{r}, \mathbf{v}) = 0$, a necessary and sufficient condition for it to remain there is given by¹⁴

$$\dot{\mathbf{r}} \cdot \frac{\partial f}{\partial \mathbf{r}} + \dot{\mathbf{v}} \cdot \frac{\partial f}{\partial \mathbf{v}} = 0 \quad (6)$$

The heating rate on the vehicle can be modeled as

$$q = C \rho^N v^M \quad (7)$$

For a local exponential density model, this may be simplified to

$$q = C \rho_0^N e^{-\beta N r} v^M = q(\mathbf{r}, \mathbf{v}) \quad (8)$$

Substituting $f = q - q_{\max}$ into Eq. (10), we get

$$\frac{\mathbf{v} \cdot \mathbf{r}}{r} \frac{\partial q}{\partial \mathbf{r}} + \frac{\dot{\mathbf{v}} \cdot \mathbf{v}}{v} \frac{\partial q}{\partial \mathbf{v}} = 0 \quad (9)$$

It is straightforward to show that Eq. (9) reduces to

$$v \sin \gamma \frac{\partial q}{\partial r} + \left(-\frac{D}{m} - g \sin \gamma + \frac{T \cos \alpha}{m} \right) \frac{\partial q}{\partial v} = 0 \quad (10)$$

Carrying out the partial derivatives, Eq. (10) finally simplifies to (for $q \neq 0$)

$$T \cos \alpha - D - m \sin \gamma (g + \xi v^2) = 0 \quad (11)$$

Equation (11) is the necessary and sufficient condition for a vehicle to maintain a constant heating rate. The condition constrains the choice of T and α over the constraint boundary. As indicated before, a widely studied profile for thrust is given by

$$T = D / \cos \alpha \quad (12)$$

and is called the aerocruise maneuver. From Eq. (11), it is clear that this choice is a valid one if and only if

$$\gamma = \dot{\gamma} = 0 \quad (13)$$

This imposition of steady state [see Eq. (1f)] yields the bank-angle control law¹⁰

$$\cos \delta = \frac{m(g - v^2/r)}{L + T \sin \alpha} \quad (14)$$

performed over a constant altitude at constant speed [cf. Eq. (1)]. In the $r-v$ space, the aerocruise phase is reduced to a single point lying on the constraint boundary. Thus an aerocruise maneuver may be broken down into three phases: 1) an unconstrained glide phase, 2) a constrained (constant-altitude) phase called aerocruise, and 3) an unconstrained boost phase. We will use the term optimal aerocruise whenever the remainder of the free controls are optimized. Thus, if Eq. (12) is an optimal solution to Eq. (11), an optimal aerocruise maneuver would be an optimal synergetic maneuver.

A simple and easy way to demonstrate the lack of optimality of a trajectory is to perform a specific control variation that lowers the cost. We choose the thrust profile [in Eq. (11)] to be simply

$$T = T_{\max} \quad (15)$$

and call it the aerobang maneuver. The angle of attack is now determined, as required by Eq. (11), by solving the nonlinear equation for α :

$$T_{\max} \cos \alpha - D(\alpha) - m \sin \gamma (g + \xi v^2) = 0 \quad (16)$$

where we have rewritten aerodynamic drag as $D(\alpha)$ to emphasize its dependence on angle of attack. Clearly, this profile imposes no additional constraints such as the one in Eq. (13) employed for the aerocruise phase. Consequently, one is free to travel over the constraint boundary. Intuitively, when a constraint is relaxed, we expect an improvement in performance. (Note that this is not a real relaxation; it is a removal of an unnecessary constraint, viz., flight

over a constant altitude.) We will assume $T_{\max} > D/\cos \alpha$ and replace the aerocruise phase by Eqs. (15) and (16) for the aerobang maneuver. In this sense, the aerobang maneuver performs a perturbation on the optimal aerocruise maneuver.

Although we may choose any hypothetical vehicle, especially one that suits to magnify the points made in the preceding analysis, we will drive home the point by choosing the entry research vehicle (ERV).^{15,16}

Numerical Results

The Program to Optimize Simulated Trajectories (POST)¹⁷ was utilized to simulate and to optimize the synergetic maneuvers. The signature aerocruise maneuver consists of a glide-cruise-bang profile. Likewise, the signature aerobang maneuver consists of a glide-constrained, bang-bang aeropass. Each of these three basic maneuvers was simulated for the ERV, whose coefficients of lift and drag are approximated by

$$C_L = 0.015 + 0.985\alpha + 0.924\alpha^2 \quad (17a)$$

$$C_D = 0.097 - 0.334\alpha + 2.619\alpha^2 \quad (17b)$$

where α is in radians. This aerodynamic model is a least-squares binomial fit of the wind-tunnel data. Table 1 provides additional useful vehicle data.¹⁵

The 1976 U.S. Standard Atmosphere, available in POST's planet module, was used for the density model. The aeroheating rates were computed using Chapman's equation¹⁷:

$$q = 9.437 \times 10^{-5} \rho^{\frac{1}{2}} v^{3.15}, \quad \text{W/m}^2 \quad (18)$$

Consistent with its design parameters,^{15,16} two heating-rate constraints were considered for the ERV: $q_{\max} = 1.41 \times 10^6 \text{ W/m}^2$ (high) and $9.6 \times 10^5 \text{ W/m}^2$ (low).

Using the preceding information, the numerically optimal solution was determined by maximizing the inclination change for a given amount of fuel. Simulations were performed for different fractions of the change in the vehicle mass, from 10 to 40%. Consistent results were obtained for all cases, and so in what follows we will discuss, in detail, the case for 30% mass fraction and summarize the rest.

To demonstrate the key points, we first benchmark the optimal aerocruise maneuver by maximizing the inclination change (for a 30% change in the vehicle mass) for a maximum heating rate of $q_{\max} = 1.41 \times 10^6 \text{ W/m}^2$. Figure 2 shows the optimal inclination profile and the associated heating-rate history. Notice that most of the inclination change takes place during the maximum heating-rate region. The optimal control histories that accompany these plots are shown in Fig. 3. As discussed in the preceding section, we now replace the aerocruise portion of the trajectory by the aerobang maneuver and redo the analysis. The aerobang inclination profile and the associated heating rates are shown in Fig. 4. It is clear that, for the same allowable maximum heating rate of 141 W/cm^2 , the perturbed maneuver, i.e., aerobang, yields a higher inclination change than aerocruise—in this case by 9.3%. The associated control profile is shown in Fig. 5. A comparison of the aerocruise and aerobang control profiles (Figs. 3 and 5) shows that the vehicle flies at lower bank angles to perform the aerocruise turn, whereas the aerobang maneuver allows the vehicle to fly at significantly higher bank angles at somewhat higher angles of attack. This is to be expected, as is apparent from Eq. (14). According to Eq. (14), as the trajectory is sub-circular (i.e., $v^2/r < g$), $\cos \delta > 0$, and hence $\delta < 90$ deg. The cen-

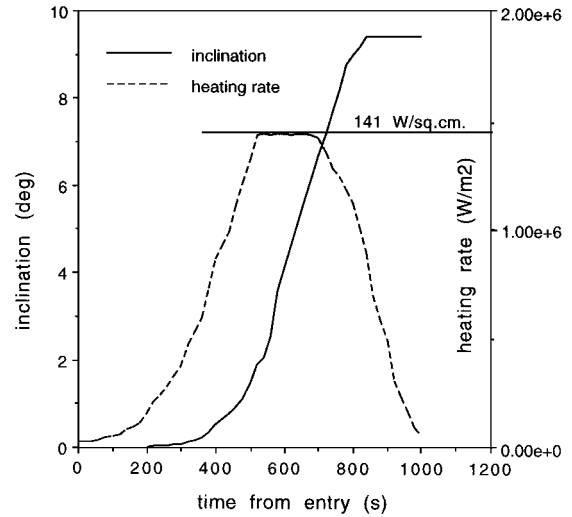


Fig. 2 Optimal inclination change and heating-rate profile for aerocruise.

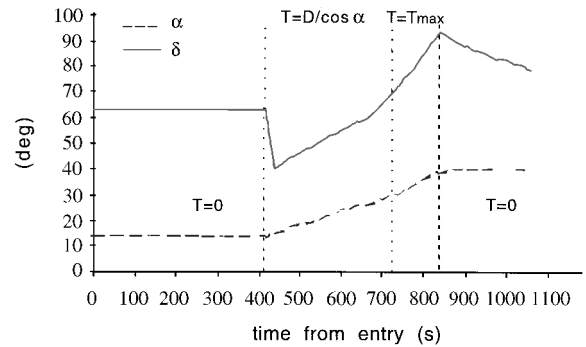


Fig. 3 Optimal control histories for aerocruise.

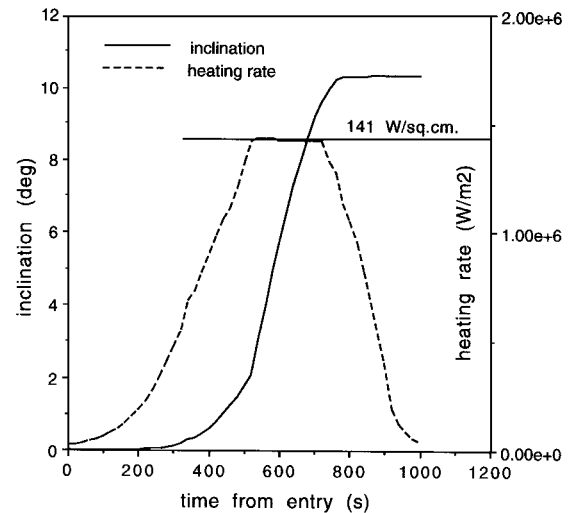


Fig. 4 Inclination change and heating-rate profile for aerobang.

Table 1 ERV data¹⁵

| Parameter | Value |
|---|-------------------------------|
| Wing reference area S , m ² | 16.48 |
| Maximum lift coefficient $C_{L_{\max}}$ | 1.153 (at $\alpha = 40$ deg) |
| Maximum lift-to-drag ratio $(L/D)_{\max}$ | 1.84 (at $\alpha = 11.9$ deg) |
| Separation mass, kg | 5,443 |
| Maximum fuel mass, kg | 2,914 |
| Thrust control authority T_{\max} , N | 14,679 |
| Specific impulse I_{sp} , s | 295 |

trifugal force alone is not sufficient to offset the gravitational force to maintain a circular flight path for the vehicle. A radial component of the lift and thrust forces is necessary to fly this constant altitude trajectory, a component that otherwise could have been used toward changing the inclination. As there is no such constraint on the aerobang maneuver, a greater portion of the binormal force may be used toward maximizing the inclination change resulting in a nonconstant altitude profile as shown in Fig. 6. This plot furthers the notion that the aerobang maneuver, as used here, produces a perturbation on the aerocruise maneuver. When the heating-rate limit is lowered to $q_{\max} = 96 \text{ W/cm}^2$, the inclination change is less (than the case for $q_{\max} = 141 \text{ W/cm}^2$), as expected, but the trend is still the same.

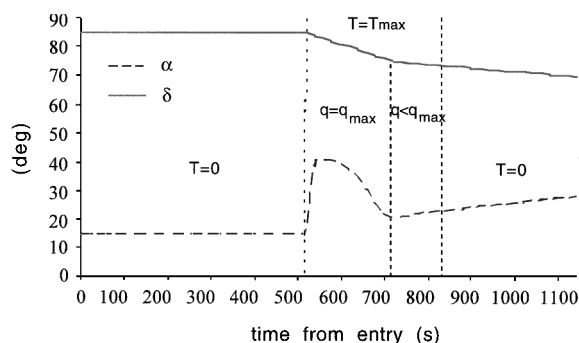


Fig. 5 Aerobang control profile.

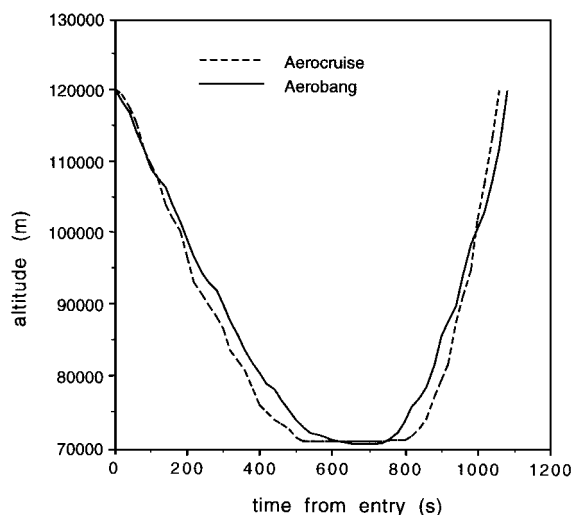


Fig. 6 Altitude profiles for aerocruise and aerobang.

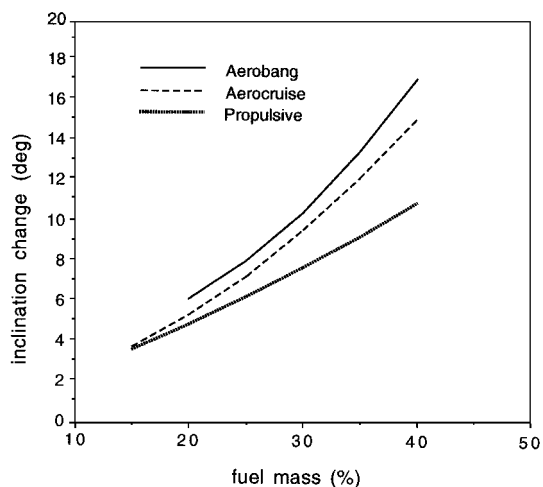


Fig. 7 Comparison of plane-change maneuvers.

When the preceding analysis was repeated for different fixed values of fuel consumption, similar results were obtained. This performance is summarized in Fig. 7, where we have included the inclination change that would be obtained for an exoatmospheric single-impulse maneuver. This consistency in performance strongly furthers the notion that the aerocruise maneuver is not an optimal synergetic maneuver.

These results show that, for the ERV, the aerobang maneuver is superior to aerocruise. The two-part question that still needs to be answered satisfactorily is what is the optimal synergetic maneuver and what does the vehicle look like when the airframe is designed with the optimal maneuver in mind? Answering the first part of the question entails a full formulation of the necessary conditions for the optimal synergetic maneuver and an exploration into the nature of the switching structure. Preliminary analysis of this problem corroborates the results of this paper, but additional work needs to

be performed to fully answer the question. The second part of the question is a multidisciplinary optimization problem that has not yet been solved.

Conclusions

This paper demonstrates that the aerocruise maneuver is not the fuel-optimal powered turn for the heating-rate-constrained synergetic maneuver. In fact, the optimal synergetic maneuver is not yet known, and it is quite possible that we may be able to obtain higher synergetic efficiencies than previously thought. Although the synergetic maneuver has been studied for quite a long time, further research is necessary to determine the optimal flight profile, such as the totality of extremal arcs, the nature of the switching structure, and the possibility of singular arcs. Armed with this information, researchers can conduct a more careful analysis of the optimal vehicle design parameters associated with the optimal synergetic maneuver.

Acknowledgments

The authors gratefully acknowledge funding provided for this research by the U.S. Naval Postgraduate School and the Air Force Space Command. We would like to thank Brian Neuenfeldt for sponsoring this research and Chris Naftel for helping us on the various intricacies of using POST. Finally, we would like to thank the anonymous reviewers for making many valuable suggestions for revising this paper.

References

- London, H. S., "Change of Satellite Orbit Plane by Aerodynamic Maneuvering," *Journal of the Aerospace Sciences*, Vol. 29, March 1962, pp. 323-332.
- Cuadra, E., and Arthur, P. D., "Orbit Plane Change by External Burning Aerocruise," *Journal of Spacecraft and Rockets*, Vol. 3, No. 3, 1966, pp. 347-352.
- Walberg, G. D., "A Survey of Aeroassisted Orbit Transfer," *Journal of Spacecraft and Rockets*, Vol. 22, No. 1, 1985, pp. 3-18.
- Mease, K. D., "Optimization of Aeroassisted Orbital Transfer: Current Status," *Journal of the Astronautical Sciences*, Vol. 36, No. 1/2, 1988, pp. 7-33.
- Menees, G. P., Brown, K. G., Wilson, J. F., and Davies, C. B., "Aerothermodynamic Heating and Performance Analysis of a High-Lift Aeromaneuvering AOTV Concept," *Journal of Spacecraft and Rockets*, Vol. 24, No. 3, 1987, pp. 198-204.
- Hsu, F.-K., Kuo, T.-S., and Chern, J.-S., "Optimal Aeroassisted Orbital Plane Change with Heating-Rate Constraint," *Journal of Guidance, Control, and Dynamics*, Vol. 13, No. 1, 1990, pp. 186-189.
- Seywald, H., "Variational Solutions for the Heat-Rate-Limited Aeroassisted Orbital Transfer Problem," *Journal of Guidance, Control, and Dynamics*, Vol. 19, No. 3, 1996, pp. 686-692.
- Ross, I. M., and Park, S.-Y., "Some Necessary Conditions for the Optimality of Synergetic Maneuvers," American Astronautical Society/AIAA Spaceflight Mechanics Meeting, AAS Paper 97-146, Huntsville, AL, Feb. 1997.
- Lee, J. Y., and Hull, D. G., "Maximum Orbit Plane Change with Heat-Transfer-Rate Considerations," *Journal of Guidance, Control, and Dynamics*, Vol. 13, No. 3, 1990, pp. 492-497.
- Mease, K. D., Lee, W. Y., and Vinh, N. X., "Orbital Changes During Hypervelocity Aerocruise," *Journal of the Astronautical Sciences*, Vol. 36, No. 1/2, 1988, pp. 103-107.
- Cervisi, R. T., "Analytic Solution for a Cruising Plane Change Maneuver," *Journal of Spacecraft and Rockets*, Vol. 22, No. 2, 1985, pp. 134-140.
- Ross, I. M., "Aerobang: A New Synergetic Plane-Change Maneuver," American Astronautical Society/AIAA Astrodynamics Conf., AAS Paper 91-418, Durango, CO, Aug. 1991.
- Vinh, N. X., *Optimal Trajectories in Atmospheric Flight*, Elsevier, Amsterdam, 1981, pp. 47-62.
- Pontryagin, L. S., Boltyanskii, V. G., Gamkrelidze, R. V., and Mischenko, E. F., *The Mathematical Theory of Optimal Processes*, Wiley-Interscience, New York, 1962, pp. 257-316.
- Powell, R. W., Naftel, J. C., and Cunningham, M. J., "Performance Evaluation of an Entry Research Vehicle," *Journal of Spacecraft and Rockets*, Vol. 24, No. 6, 1987, pp. 489-495.
- Freeman, D. C., Powell, R. W., Naftel, J. C., and Wurster, K. E., "Definition of an Entry Research Vehicle," *Journal of Spacecraft and Rockets*, Vol. 24, No. 3, 1987, pp. 277-281.
- Brauer, G. L., Cornick, D. E., and Stevenson, R., "Capabilities and Applications of the Program to Optimize Simulated Trajectories (POST)," NASA CR-2770, Feb. 1977.